A Highly Expressing, Soluble, and Stable Plant-Made IgG Fusion Vaccine Strategy Enhances Antigen Immunogenicity in Mice Without Adjuvant

Andrew G. Diamos[1,2]*, Mary D. Pardhe[1,2], Haiyan Sun[1,2], Joseph G. L. Hunter[1,2], Jacquelyn Kilbourne[1,2], Qiang Chen[1,2] and Hugh S. Mason[1,2]*

[1] Center for Immunotherapy, Vaccines, and Virotherapy, Biodesign Institute, Arizona State University, Tempe, AZ, United States,
[2] School of Life Sciences, Arizona State University, Tempe, AZ, United States

Therapeutics based on fusing a protein of interest to the IgG Fc domain have been enormously successful, though fewer studies have investigated the vaccine potential of IgG fusions. In this study, we systematically compared the key properties of seven different plant-made human IgG1 fusion vaccine candidates using Zika virus (ZIKV) envelope domain III (ZE3) as a model antigen. Complement protein C1q binding of the IgG fusions was enhanced by: 1) antigen fusion to the IgG N-terminus; 2) removal of the IgG light chain or Fab regions; 3) addition of hexamer-inducing mutations in the IgG Fc; 4) adding a self-binding epitope tag to create recombinant immune complexes (RIC); or 5) producing IgG fusions in plants that lack plant-specific β1,2-linked xylose and α1,3-linked fucose N-linked glycans. We also characterized the expression, solubility, and stability of the IgG fusions. By optimizing immune complex formation, a potently immunogenic vaccine candidate with improved solubility and high stability was produced at 1.5 mg IgG fusion per g leaf fresh weight. In mice, the IgG fusions elicited high titers of Zika-specific antibodies which neutralized ZIKV using only two doses without adjuvant, reaching up to 150-fold higher antibody titers than ZE3 antigen alone. We anticipate these findings will be broadly applicable to the creation of other vaccines and antibody-based therapeutics.

Keywords: Zika virus, vaccine, envelope domain, IgG fusion, recombinant immune complex, C1q, transient expression, plant-made

HIGHLIGHTS

- A modified immune complex has high expression, solubility, stability, and immunogenicity.
- Antigen immunogenicity is improved up to 150-fold by fusion to plant-made IgGs.
- High serum IgG titers >1:500,000 were achieved with only two doses without adjuvant.

INTRODUCTION

Subunit vaccines consisting of recombinant protein antigens are very promising due to their safety, ease of production, and capacity to elicit targeted immune responses directed towards desired epitopes. However, when delivered by themselves, these antigens often fail to generate robust and long-lasting immune responses, necessitating strategies to enhance their immunogenicity (1). Protein fusions to a variety of bioengineered IgG-based scaffolds have demonstrated tremendous potential as therapeutic candidates, acting to enhance the solubility and stability of the fusion partner while also allowing simple and cost-effective purification via protein A/G affinity chromatography (2). Furthermore, by interacting with neonatal Fc receptors (FcRn) in the body, IgG fusions can escape lysosomal degradation, thereby extending the serum half-life of the Fc-fusion (3).

Though less well explored, IgG fusions also have many desirable characteristics for vaccine development. Antigen-presenting cells can uptake and process IgG-bound antigen via FcRn receptors (4, 5), complement receptor C1q (6–8) and Fcγ receptors (9). However, not all IgG subclasses interact equally with immune receptors. IgG1 and IgG3 are immunostimulatory, while IgG2 and IgG4 have weak effector functions (10). IgG3 mediates the strongest complement activation and Fc receptor binding, however it has significantly reduced serum half-life, and thus most IgG-fusions vaccine strategies use human IgG1 (11). In addition to these factors, the polymeric state of an antibody also affects its immunological properties. Both C1q, the first component involved in complement activation, and the low affinity Fcγ receptors require high avidity binding for activation. For this reason, monovalent Fc-antigen fusions cannot efficiently utilize these pathways. By contrast, larger antigen-antibody immune complexes with multivalent Fc domains can efficiently bind C1q and cross-link Fc receptors, resulting in greatly improved uptake and presentation by dendritic cells, and subsequently improved activation of T-cells (6, 12–14).

Capitalizing on the benefits of antigen-antibody immune complexes, a variety of vaccine strategies have been developed to improve antigen immunogenicity. Immune complexes have been used to focus the immune response towards favorable antigenic sites (15, 16) as well as enhance the potency and breadth of the immune response by selecting for high affinity B-cells (17). By engineering antigen-IgG fusions to form polymeric structures via inclusion of the IgM tailpiece, both humoral and cellular immune responses were enhanced in the absence of adjuvant (18, 19). While traditional immune complexes consisting of antigen mixed with antibody will form variable structures depending on the oligomeric status of the antigen, we and others have developed a recombinant immune complex (RIC) strategy that allows consistent formation of large immune complexes which can efficiently engage complement (20). In the RIC system, a well-characterized antibody is tagged with its own binding site and is fused to an antigen of choice. The resulting molecules self-interact and form highly immunogenic antigen-antibody clusters. Past research has shown the potential for RIC-like molecules to produce promising vaccine candidates for *Clostridium tetani* (21), Ebola virus (22, 23), *Mycobacterium tuberculosis* (24), dengue virus (25), human papillomavirus (26) and Zika virus (27).

Zika virus (ZIKV) envelope domain III (ZE3) is a promising subunit vaccine candidate due to its ability to generate neutralizing antibodies without potential for antibody-dependent enhancement (28–30). However, like many subunit vaccines consisting of viral antigens, it is not strongly immunogenic on its own, necessitating high doses with adjuvant and repeated immunizations (30). We have previously shown that RIC carrying ZE3 elicits strong immune responses (27). However, traditional RIC may be undesirable, as the large complex size renders them poorly soluble and limits their viability as a vaccine candidate (26). Therefore, in this study we built on recent advances in antibody engineering to design and explore a panel of modified IgG fusion vaccines carrying ZE3 as a model antigen. These constructs contained modifications designed to alter their polymeric and C1q binding characteristics. We then compared the C1q binding, expression, solubility, stability, and immunogenicity of the IgG fusions.

EXPERIMENTAL PROCEDURES

Vector Construction

The construction of a geminiviral replicon plant expression vector for ZE3, as well as its fusion to the 6D8 C-terminus (pBYR11eM-h6D8ZE3, referred to here as construct "HLZe") or N-terminus with epitope tag (pBYR11eMa-BAZE3-Hgp371) or without epitope tag (pBYR11eMa-BAZE3-H) have been previously described (27, 31) A vector pBYKEMd2-6D8 expressing the full 6D8 mAb without ZE3 fusion (construct "HL") has been previously described (27, 31). To create a vector expressing only the light chain of 6D8, pBYKEMd2-6D8 was digested with XhoI and the vector was self-ligated to yield pBYKEMd-6D8K. A vector expressing only the heavy chain of

6D8 (construct "H") was created by digesting pBYKEMd2-6D8 with SacI and self-ligating the vector, to yield pBYKEMd-6D8H. The 6D8 epitope binding tag was added to pBYKEMd-6D8H by digesting pBYR11eMa-BAZE3-Hgp371 with BsaI-SacI and inserting the tag-containing fragment into pBYKEMd-6D8H digested with BsaI-SacI, yielding pBYKEMd-6D8Hgp371 (construct "HLe" when coexpressed with light chain). To remove the epitope tag from HLZe, pBYR11eM-h6D8ZE3 was digested with BamHI-SacI and ligated with a fragment containing ZE3 obtained *via* amplification with primers ZE3-Bam-F (5'-gcgggatccaagggcgtgtcatactcc) and ZE3-Sac-R (5'-acagagctcttaagtgctaccactcctgtg) and subsequent digestion with BamHI-SacI. The resulting vector, pBYKEMd-HZE3, was coinfiltrated with pBYKEMd-6D8K to produce construct "HLZ." To produce ZE3 fused to the 6D8 N-terminus without light chain, pBYR11eMa-BAZE3-H was digested with SacI and the vector vector was self-ligated, yielding pBYKEMd-ZE3H (construct "ZH"). To introduce hexamer mutations, a region of the 6D8 heavy chain constant region was synthesized (Integrated DNA Technologies, Iowa, USA) containing the E345R, E430G, and S440Y mutations, then digested with BsaI-SacI and used to replace the BsaI-SacI region of 6D8 in pBYKEMd-ZE3H, yielding pBYKEMd-ZE3Hx (construct "ZHx"). RIC epitope tag mutant "a" was generated by annealing oligos 6D89-F (5'-ctagtgtttacaagctggacatatctgaggcataagagct) and 6D89-R (5'-cttatgcctcagatatgtccagcttgtaaaca) and ligating them into pBYR11eM-h6D8ZE3 digested SpeI-SacI; mutant "b" was generated by first amplifying mutant "a" with primers gpDISE-Sac-R: (5'-tttgagctcttactcagatatgtccagcttgtaaac) and 35S-F (5'aatcccactatccttcgc), then digesting the product with SpeI-SacI and ligating it into pBYR11eM-h6D8ZE3 digested with SpeI-SacI. Mutants "c" and "d" were created similarly to mutant "a" using overlapping oligos 6D87-F (5'-ctagttacaa gctggacatatctgagtaagagct) and 6D87-R (5'-cttactcagatatgtcc agcttgtaa) for "c" and 6D86-F (5'-ctagttacaagctggacatatcttaa gagct) and 6D86-R (5'-cttaagatatgtccagcttgtaa).

In order to make a construct in which the variable heavy (VH) domain is linked to a variable light chain (VL) domain that, in turn, is directly fused to the constant region of the 6D8 antibody, the variable regions were first obtained through PCR amplification and end-tailoring of segments from pBYR11eM-h6D8ZE3. For the VH domain, the primers LIR-H3A (5'-aagcttgttgttgtgactccgag) and 6D8VH-Spe-R (5' cggactagtag ctgaagacactgtgac) were used. The VL region was obtained through PCR amplification of pBYR11eM-h6D8ZE3 with primers 35S-F (5'-aatcccactatccttcgc) and 6D8VK-Nhe-R (5'-cgtgctagccttgatctccactttggtc). In order to fuse VL region to the constant region of a human IgG antibody, a subclone was created by digesting the PCR fragment with XhoI-NheI and inserting it into a vector, pKS-HH-gp371, that contained the 6D8 heavy chain (Kim et al., 2015). This subclone was named pKS-VL. Next, pBYKEM-6D8K was digested with SbfI-SacI, the PCR product that amplified the variable heavy chain fragment was digested SbfI-SpeI, and the variable light chain subclone was digested SpeI-SacI. These fragments were assembled to create pBYKEMd2-VHLVK (construct "HVL"). Finally, this construct was used to create pBYKEMd2-HVLZe by a two-fragment ligation. The pBYKEMd2-VHLVK construct was digested BsaI and SacI to obtain the vector fragment along with the variable regions of the heavy and light chains. To obtain the ZE3 antigen segment and the epitope tag, pBYR11eM-h6D8ZE3 was also digested BsaI-SacI. The resulting construct, which was used to produce HVLZe, was named pBYKEMd-HVLZe.

Agroinfiltration of *Nicotiana benthamiana* Leaves

Binary vectors were separately introduced into *Agrobacterium tumefaciens* EHA105 by electroporation. The resulting strains were verified by restriction digestion or PCR, grown overnight at 30°C, and used to infiltrate leaves of 5- to 6-week-old *N. benthamiana* maintained at 23°C to 25°C. Briefly, the bacteria were pelleted by centrifugation for 5 min at 5,000g and then resuspended in infiltration buffer (10 mM 2-(N-morpholino) ethanesulfonic acid (MES), pH 5.5 and 10 mM MgSO4) to OD600 = 0.2, unless otherwise described. The resulting bacterial suspensions were injected by using a syringe without needle into leaves through a small puncture (32). To evaluate the effects of glycosylation, transgenic plants silenced for xylosyltransferase and fucosyltransferase were employed (33). Plant tissue was harvested at 5 days post infiltration (DPI).

Protein Extraction, Expression, and Purification

Crude protein was extracted by homogenizing agroinfiltrated leaf samples with 1:5 (*w:v*) ice cold extraction buffer (25 mM Tris-HCl, pH 8.0, 125 mM NaCl, 3 mM EDTA, 0.1% Triton X-100, 10 mg/ml sodium ascorbate, 0.3 mg/ml phenylmethylsulfonyl fluoride) using a Bullet Blender machine (Next Advance, Averill Park, NY) following the manufacturer's instruction. Homogenized tissue was rotated at 4°C for 30 min. The crude plant extract was clarified by centrifugation at 13,000g for 15 min at 4°C and the supernatant was analyzed by SDS-PAGE or ELISA. Alternatively, to evaluate solubility of proteins in the original homogenate, the pellet was designated the insoluble fraction and treated with SDS sample buffer at 100°C for 10 min before loading on SDS-PAGE.

IgG variants were purified by protein G affinity chromatography. Agroinfiltrated leaves were blended with 1:3 (w:v) ice cold extraction buffer (25 mM Tris-HCl, pH 8.0, 125 mM NaCl, 3 mM EDTA, 0.1% Triton X-100, 10 mg/ml sodium ascorbate, 0.3 mg/ml phenylmethylsulfonyl fluoride), stirred for 30 min at 4°C, and filtered through miracloth. To precipitate endogenous plant proteins, the pH was lowered to 4.5 with 1M phosphoric acid for 5 min while stirring, then raised to 7.6 with 2M Tris base. Following centrifugation for 20 min at 16,000g, the clarified extract was loaded onto a Protein G column (Thermo Fisher Scientific, Waltham, MA, USA) following the manufacturer's instructions. Purified proteins were eluted with 100 mM glycine, pH 2.5, directly into collection tubes containing 1M Tris-HCl pH 8.0 to neutralize the elution buffer and stored at −80°C. Purified protein concentration was measured by A280 absorbance, ELISA, and gel quantification.

ZE3-His expressed from pBYe3R2K2Mc-BAZE3 was purified by metal affinity chromatography. Protein was extracted as described above, but without acid precipitation. The clarified extract was loaded onto a column containing TALON Metal Affinity Resin (BD Clontech, Mountain View, CA) according to the manufacturer's instructions. The column was washed with PBS and eluted with elution buffer (PBS, 150 mM imidazole, pH 7.4). Peak ZE3 elutions were pooled, dialyzed against PBS, and stored at −80°C.

SDS-PAGE and Western Blot

Plant protein extracts or purified protein samples were mixed with SDS sample buffer (50 mM Tris-HCl, pH 6.8, 2% SDS, 10% glycerol, 0.02% bromophenol blue) and separated on 4% to 15% stain-free polyacrylamide gels (Bio-Rad, Hercules, CA, USA). For reducing conditions, 0.5M DTT was added, and the samples were boiled for 10 min prior to loading. Polyacrylamide gels were visualized and imaged under UV light, then transferred to a PVDF membrane. For IgG detection, the protein transferred membranes were blocked with 5% dry milk in PBST (PBS with 0.05% tween-20) overnight at 4°C and probed with goat anti-human IgG-HRP (Sigma-Aldrich, St. Louis, MO, USA diluted 1:5000 in 1% PBSTM). Bound antibody was detected with ECL reagent (Amersham, Little Chalfont, United Kingdom).

ELISA Quantification of Construct Expression Levels

For ZE3 ELISA, 96-well high-binding polystyrene plates (Corning Inc, Corning, NY, USA) were coated with a 1:500 dilution of unlabeled goat anti-human IgG (Southern Biotech, Birmingham, AL, USA) and incubated at 37°C for 1 h. After being washed with PBST, the plates were blocked with 5% non-fat dry milk in PBST for 30 min and washed with PBST. Multiple dilutions, ranging from 1:100 to 1:25,000, of clarified plant extracts containing the different constructs were added to the plates. Previously purified and quantified plant-produced HLZ was included as a standard and positive control while samples of uninfiltrated crude extract were added for a negative control. After a 1-h incubation, the plates were washed three times in 1× PBST. Plates were then incubated with a 1:1000 dilution of mouse serum raised against ZE3-6H followed by goat anti-mouse IgG HRP conjugate (Southern Biotech, Birmingham, AL, USA) for 1 h at 37°C. The plates were then washed five times with PBST, developed with TMB substrate (Thermo Fisher Scientific, Waltham, MA, USA), and the absorbance read at 450 nm. IgG ELISA was performed similarly, except constructs were bound directly to the plates and detected with goat anti-mouse IgG HRP conjugate (Southern Biotech, Birmingham, AL, USA).

C1q Binding and FcγRIII Binding

96-well high-binding polystyrene plates (Corning Inc, Corning, NY, USA) were coated with 15 µg/ml human complement C1q (PFA, MilliporeSigma, MA) in PBS for 2 h at 37°C. The plates were washed three times with PBST, and then blocked with 5% dry milk in PBST for 15 min. After washing three times with PBST, purified human IgG (Southern Biotech, Birmingham, AL, USA) and purified IgG-ZE3 fusions were added at 0.1 mg/ml

with 10-fold serial dilutions and incubated for 1.5 h at 37°C. After washing three times with PBST, bound IgG was detected by incubating with 1:1000 polyclonal goat anti human IgG-HRP (Southern Biotech, Birmingham, AL, USA) for 1 h at 37°C. The plates were washed 4 times with PBST, developed with TMB substrate (Thermo Fisher Scientific, Waltham, MA, USA), stopped with 1M HCl, and the absorbance was read at 450 nm.

To test FcγRIII binding, a 96-well high-binding polystyrene plate (Corning Inc, Corning, NY, USA) was coated with 1.2 µg/ml human FcγRIIIA/CD16a protein (BioLegend, San Diego, CA, USA) in PBS for 1 h at 37°C. The plate was washed three times with PBST and then blocked with 5% dry milk in PBST for 30 min. After washing three times with PBST, purified constructs were added at equimolar concentrations. The starting concentrations of the proteins were as follows: HLZe at 18 µg/ml, HLZ at 17.5 µg/ml; and HL at 15 µg/ml. These and 10-fold dilutions of each were applied to the wells and incubated overnight at 4°C. After washing three times with PBST, the bound constructs were detected by incubating the plate with a 1:500 dilution of an anti-human IgG (whole molecule) HRP-labeled probe (Sigma-Aldrich, St. Louis, MO, USA) for 1 h at 37°C. The plate was washed 4 times with PBST, developed with TMB substrate (Thermo Fisher Scientific, Waltham, MA, USA), stopped with 1M HCl, and the absorbance was read at 450 nm.

6D8 Epitope Binding

To test the ability of HVL to bind to the 6D8 epitope tag, 900 ng of purified dengue consensus envelope domain III tagged with 6D8 epitope (25) were bound to a 96-well high-binding polystyrene plate (Corning Inc, Corning, NY, USA). After a 1-h incubation at 37°C, the plate was washed thrice with PBST and blocked with 5% dry milk in PBST for 30 min. Then, the plate was washed thrice with PBST and various dilutions of either purified HLV or full-length 6D8 antibody were added to the plate. The plate was incubated at 37°C for 1 h, washed thrice with PBST and detected with HRP-conjugated mouse anti-human IgG (Fc only) (Southern Biotech, Birmingham, AL, USA) antibody at a 1:2000 dilution. Then, the plate was thoroughly washed with PBST and developed with TMB substrate (Thermo Fisher Scientific, Waltham, MA, USA). The absorbance was read at 450 nm.

Sucrose Gradient Density Centrifugation

Purified samples of each IgG fusion (100 µl) were loaded onto discontinuous sucrose gradients consisting of 350 µl layers of 5, 10, 15, 20, and 25% sucrose in PBS in a 2.0 ml microcentrifuge tubes and centrifuged at 21,000g for 16 h at 4 °C. Fractions were collected from the top and analyzed by SDS-PAGE, followed by visualization on stain-free gels (Bio-Rad, Hercules, CA, USA). The relative band intensity of each fraction was determined using ImageJ software, with the peak band arbitrarily assigned the value of 1.

Stability of IgG Fusions During Storage

After purification, samples of purified IgG fusions were frozen at −80°C. Samples were either untreated (referred to as "initial"), or thawed and then subjected to either five additional freeze/thaw

cycles, or incubated for 2 weeks at 4°C, or incubated for 2 weeks at 23°C. Initial and treated samples were visually inspected for any signs of precipitation, and then analyzed by reducing and non-reducing SDS-PAGE to observe cleavage of ZE3 or other degradation products. ImageJ analysis was used to compare the band intensity of the fully formed product to that of any degradation products. Each sample was also analyzed as described in section 4.6 for C1q binding.

Immunization of Mice and Sample Collection

All animals were handled in accordance to the Animal Welfare Act and Arizona State University IACUC under study number 18-1616R. Female BALB/C mice, 6 to 8 weeks old, were immunized subcutaneously with purified IgG fusion variants. In all treatment groups, the total weight of antigen was set to deliver an equivalent 8 µg of ZE3. Doses were given on days 0 and 14. Serum collection was done as described (34) by submandibular bleed on days 0, 14, and 28.

Antibody Measurements

Mouse antibody titers were measured by ELISA. Plant-expressed 6-His tagged ZE3 at 50 ng/well was bound to 96-well high-binding polystyrene plates (Corning Inc, Corning, NY, USA), and the plates were blocked with 5% nonfat dry milk in PBST. After washing the wells with PBST (PBS with 0.05% Tween 20), the mouse sera were diluted with 1% PBSTM (PBST with 1% nonfat dry milk) and incubated. Mouse antibodies were detected by incubation with polyclonal goat anti-mouse IgG-horseradish peroxidase conjugate (Sigma-Aldrich, St. Louis, MO, USA). The plate was developed with TMB substrate (Thermo Fisher Scientific, Waltham, MA, USA), stopped with 1M HCl, and the absorbance was read at 450 nm. Endpoint titers were taken as the reciprocal of the lowest dilution which produced an OD_{450} reading twice the background produced using PBS as the sample. IgG2a antibodies were measured from sera diluted 1:100 in 1% PBSTM and detected with IgG2a horseradish peroxidase conjugate (Santa Cruz Biotechnology, Dallas, TX, USA). IgG2a values were normalized by total IgG, and the value obtained for ZE3 was arbitrarily defined as 1.0. The ratios for each construct were calculated as IgG2a:IgG values relative to that of ZE3.

Plaque Reduction Neutralization Assay

Serum samples from terminal blood collection were pooled for each mouse group and heat inactivated. As described previously (35), the PRNT assay was carried out using mouse sera diluted in Opti-Mem media (Invitrogen) at ratio of 1:10. Each sample was incubated with 100 pfu ZIKV (PRVABC59, ATCC# VR-1843) in equal volume for 1 h at 37°C before the virus/serum mixture was added to each well of VERO cells (ATCC # CCL-81) in a 24 well plate. The virus/serum mixture was aspirated after a 1.5-h incubation at 37°C. Subsequently, VERO cells were overlaid with 0.8% agarose in DMEM medium containing 5% FBS (Invitrogen, CA) and incubated at 37°C for three days. Finally, VERO cells were fixed with 4% paraformaldehyde (PFA, MilliporeSigma, MA) overnight and stained with 0.2% crystal violet. Plaques from each well were counted and neutralization % was calculated by using the formula: [(number of ZIKV plaque per well in virus only control wells)-(number of ZIKV plaque per well of diluted serum)/(number of ZIKV plaque per well in virus only control wells) x 100]. Neutralizing titers >10 refer to constructs with >50% neutralization at a 1:10 serum dilution.

RESULTS

Modified Plant-Made IgG-ZE3 Fusions Exhibit Variable Binding to Complement Receptor C1q

We designed a panel of human IgG1 variants based on the previously characterized humanized anti-Ebola monoclonal antibody 6D8 (22) fused to ZE3 (**Figure 1A**). A RIC construct was created by fusing 6D8 epitope-tagged ZE3 *via* a flexible linker to the C-terminus of the 6D8 heavy chain. When in solution, the 6D8 Fab arms of one 6D8-ZE3 fusion molecule bind the epitope-tagged ZE3 on another fusion molecule, forming antigen-antibody clusters (20). This RIC construct is referred to as "HLZe" as it contains the 6D8 **H**eavy chain, 6D8 **L**ight chain, C-terminal **Z**E3 fusion, and 6D8 **e**pitope binding tag. As a control for immune complex formation, an otherwise identical construct was created without the epitope tag (construct "HLZ"). This construct would not be expected to form immune complexes as it cannot specifically bind other HLZ molecules. The 6D8 antibody without ZE3 or epitope tag is referred to as construct "HL," and the corresponding RIC with epitope tag but lacking ZE3 is referred to as "HLe." Since C1q mediates immune complex uptake into antigen presenting cells and complement-coated immune complexes play a key role in activating and maintaining long-term immunity (7, 8, 36, 37), the constructs were analyzed for C1q binding. Additionally, C1q binding provides insight into the polymeric status of the constructs, as RIC and other polymeric IgGs have stronger binding to C1q when compared with monomeric IgG (18, 21). To improve C1q binding, all constructs were expressed in glycoengineered *Nicotiana benthamiana* that have suppressed fucosyl- and xylosyl transferase activities, as these glycans inhibit immune receptor binding (38). HL or HLe made in glycoengineered plants showed highly improved C1q binding compared to constructs expressed in wildtype plants (**Figure S1A**). Consistent with the formation of densely clustered antigen-antibody complexes, HLZe showed greatly improved C1q binding compared to HLZ (p < 0.001) (**Figure 1B**). A small increase in C1q binding was noted with HLZ compared to HL (p < 0.05) (**Figure 1B**), suggesting low-level aggregation of the construct or slight favorable alteration of Fc conformation due to the ZE3 fusion. HLZe also efficiently bound FcγRIIIa, exceeding the binding of HLZ and HL (**Figure S1B**).

Hexamers are the ideal substrate for C1q binding (39) and it has been suggested that the antibody Fab arms play a regulatory role in complement activation by inhibiting C1q binding (40). Upon addition of certain soluble antigens or removal of the light chains, C1q binding is dramatically improved, suggesting
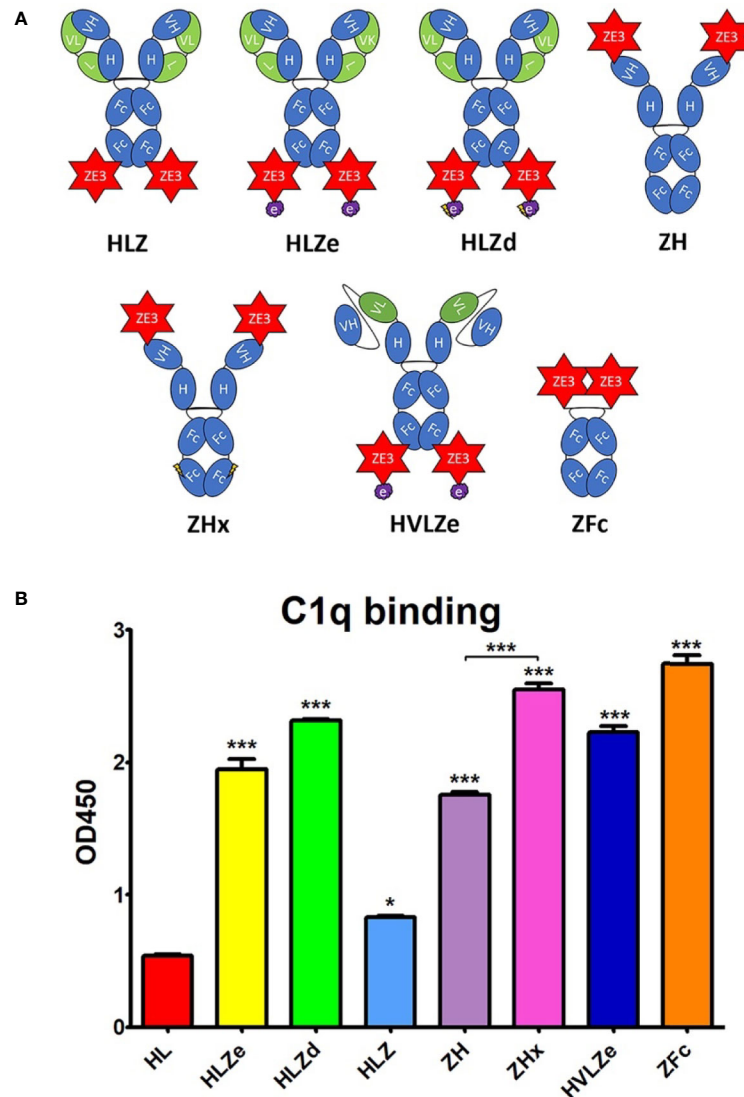
FIGURE 1 | Various IgG fusion strategies enhance C1q binding **(A)**. Schematic representation of IgG fusion constructs used in this study. Fusion constructs are built on the mAb 6D8 human IgG1 backbone with the shown modifications. ZE3; the Zika envelope domain III containing amino acids K301 to T406; e, an epitope tag containing the "VYKLDISEA" 6D8 binding motif for RIC formation; e with lightning bolt, an epitope tag truncated to include only "YKLDIS" to reduce RIC formation; VH, the variable heavy domain from 6D8 which participates in binding the epitope tag; VL, the variably light domain from 6D8 which participates in binding the epitope tag; H, the heavy chain constant CH1 domain from 6D8; L, the light chain constant domain from 6D8; Fc, the heavy chain constant CH2 or CH3 domains from 6D8; Fc with lightning bolt, same as Fc but with E345R, E430G, and S440Y mutations to induce hexamer formation **(B)**. C1q binding ELISA of purified IgG fusion constructs made in plants that lack plant-specific β1,2-linked xylose and α1,3-linked fucose N-linked glycans. ELISA plates were coated with 15 μg/ml human C1q and incubated with 10 μg/ml each molecule, using 6D8 with no fusion as a negative control. Constructs were detected using polyclonal goat anti-human IgG-HRP. Mean OD_{450} values from three samples are shown ± standard error with one star (*) indicating $p < 0.05$ and three stars (***) indicating $p < 0.001$ as measured by one-way ANOVA comparing each column to the control column HL, unless otherwise indicated with a bracket.

conformational changes are conveyed into the Fc domain from the Fab arms to induce hexamer formation (40). In agreement with this model, we find that the addition of soluble antigen carrying the 6D8 epitope tag modestly improved C1q binding (**Figure S2**, compare HL vs HL + Ag) and C1q binding was strongly enhanced by removal of the antibody light chain (**Figure S2**, compare HL and H). Interestingly, antigen fusion to the heavy chain N-terminus also strongly improved C1q

binding at a level similar to removing the light chain (**Figure S2**, compare HL, H, and ZHL). Therefore, we created a construct with ZE3 fused to the N-terminus of the heavy chain (construct "ZH") in the absence of the light chain. ZH efficiently bound C1q similar to HLZe; however, the effects of light chain removal and N-terminal ZE3 fusions were not additive (**Figure 1B**). In an attempt to further improve interaction with C1q, we made a construct that was similar to ZH except for mutations E345R,

E430G, and S440Y in the Fc region which favor formation of hexamers (39). This construct (ZHx) had modestly improved C1q binding compared to ZH (p < 0.001) (**Figure 1B**). Past studies have shown that IgG1 Fc fusions (lacking VH and CH1 domains) produce variable levels of C1q binding depending on the fusion partner (41). However, Fab arm removal can favor hexamer formation with strong complement activation (40). ZE3 N-terminally fused to the 6D8 Fc (**Figure 1A** construct "ZFc") showed very strong C1q binding (**Figure 1B**). Finally, as RIC require co-expression of heavy and light chains, we constructed a simplified RIC that consisted of a single chain antibody with the variable light (VL) domain of 6D8 inserted between the variable heavy (VH) and CH1 domains of 6D8 to yield construct "HVL". This construct bound antigen tagged with the 6D8 epitope, albeit at a somewhat reduced level compared to unaltered 6D8 (**Figure S3**). This single-chain Fab configuration was fused to ZE3 to create the single chain RIC HVLZe (**Figure 1A**), which displayed strong C1q binding (**Figure 1B**). Together, these data demonstrate that RIC formation, removal or rearrangement of light chain/Fab region, Fc hexamer mutations, and ZE3 fusion to the IgG N-terminus all increase C1q binding of plant-made IgG1.

Reducing RIC Self-Binding Improves Solubility Without Reducing C1q Binding

RIC suffer from low yield of soluble product (26). While unmodified 6D8 antibody is highly soluble, addition of the short epitope tag (construct HLe) renders the antibody mostly insoluble (**Figure S4**). However, this is prevented by removal of the light chain (construct He), which is needed for epitope binding (25), suggesting that the insolubility arises from large complexes of antibody bound to the epitope tag (**Figure S4**). To improve RIC solubility, we shortened the 6D8 epitope tag in order to reduce the strength of self-binding. Construct "HLa" contains the minimal reported binding region for 6D8 "VYKLDISEA" (42). Removal of a single amino acid from the C-terminus (construct "HLb," epitope VYKLDISE) had no effect on solubility (**Figure S5A**). However, further removal of a single amino acid from the N-terminus (construct "HLc," YKLDISE), and additional truncation in construct "HLd" (YKLDIS) resulted in greatly improved solubility, yielding 20-fold more soluble antibody (**Figure S5B**). Thus, the truncated epitope present in HLd was introduced to HLZe (construct HLZd) and characterized. Despite reducing epitope binding compared to full length epitope tag by approximately 25-fold by ELISA (**Figure S5C**), HLZd still maintained very strong C1q binding, suggesting efficient complex formation still remained (**Figure 1B**). Note that the otherwise identical construct HLZ, which lacks the YKLDIS tag, had 10-fold lower C1q binding (**Figure S5D**). These data suggest that RIC solubility can be enhanced by reducing self-binding without a loss of C1q activation.

Highly Variable Expression and Solubility of IgG Fusions in Plants

Since a viable vaccine candidate must be soluble and highly expressing, we measured the soluble yield of fully assembled IgG

fusions by employing an ELISA assay that first captured ZE3 and then detected human IgG. As a standard, purified and quantified HLZ was used. To detect any proteolytic cleavage of ZE3, an ELISA measuring total IgG irrespective of the presence of ZE3 was also used as a comparison, using purified and quantified unfused HL as standard. When soluble extracts were probed for the presence of both ZE3 and IgG, construct ZH yielded 0.83 mg fully formed product per gram leaf fresh weight (mg/g LFW), and the similar ZFc yielded 0.58 mg/g LFW (**Figure 2A**). However, when measuring the total IgG content, the yield of ZH was roughly 1.2-fold higher and, for ZFc, 2.5-fold higher than ZE3 ELISA, which suggests that ZH and especially ZFc are susceptible to proteolytic cleavage. This finding was confirmed by visualization of the ZFc cleavage products on SDS-PAGE (**Figure 2B**). HLZ accumulated only 0.17 mg/g LFW fully assembled product, with roughly 40% ZE3 lost to cleavage, suggesting general instability of the construct (**Figures 2A, B**). By ELISA, the polymeric RIC constructs seemingly had lower yields than the monomeric constructs: HLZe and HLZd only accumulated 0.04 mg/g LFW and 0.30 mg/g LFW respectively, and the hexameric ZHx accumulated only 0.08 mg/g LFW (**Figure 2A**). However, when visualized under reducing SDS-PAGE conditions, HLZd was the highest expressing construct, accumulating an estimated 1.5 mg/g LFW, over twice the highest yield of the next best construct, with no visible degradation products (**Figures 2A, B**). The discrepancy between ELISA and gel quantification likely arises due to complexed HLZd being less accessible to the antibody probe by ELISA. Importantly, the gel quantification results agreed with the ELISA results for all the monomeric constructs, but not for any of the polymeric constructs (**Figure 2A**). Thus, the total yield of HLZe and ZHx was also higher when measured by gel quantification (**Figures 2A, B**). While polymeric constructs were partially inaccessible to the antibody probe by traditional ELISA (**Figure 2A**), they were strongly detected using the same antibody probe in the C1q assay (**Figure 1B**). This likely occurred due to C1q disaggregating the polymeric constructs, as C1q functions to solubilize immune complexes *in vivo* (43). Construct HVLZe yielded only 0.02 mg/g LFW soluble product by ELISA and was not visible by SDS-PAGE (**Figure 2A**). However, we detected very high levels when extracting with 7.5 M urea (data not shown) suggesting that the construct insolubility resulted in the low yield. In total, these results show that the different IgG fusions display expression levels which vary by several orders of magnitude, highlighting the large differences in their capacity to be used as viable, affordable vaccines.

Purification and Aggregation of IgG Fusion Constructs

IgG fusions were purified to >95% homogeneity using a simple one-step purification *via* protein G affinity chromatography. In agreement with the expression data, the more polymeric constructs showed less degradation than the other constructs, and the ZFc fusion had particularly high levels of degradation (**Figure 3**). To investigate the polymeric characteristics of each construct, purified IgG fusions were analyzed by sucrose gradient
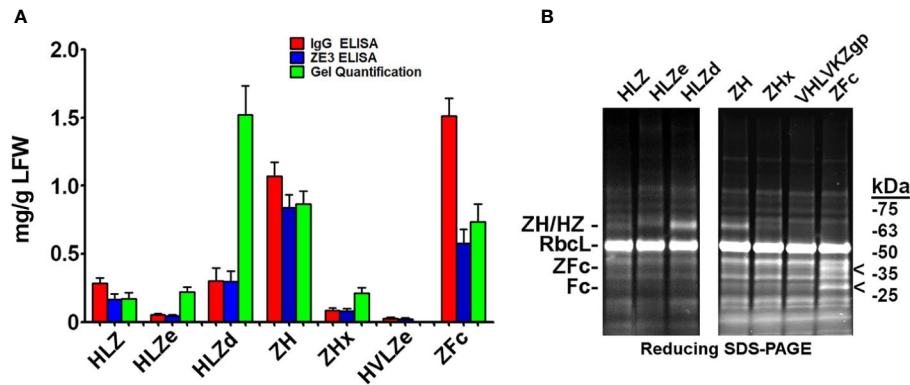
FIGURE 2 | Modified IgG fusions have improved expression and solubility **(A)**. ELISA and gel quantification of IgG fusion construct expression. Clarified protein extracts ("soluble" fraction) from leaf spots agroinfiltrated with each IgG fusion construct were analyzed by either ELISA, or SDS-PAGE followed by gel image quantification. For ZE3 ELISA, plates were coated with polyclonal mouse anti-ZE3, incubated with serial dilutions of extracts from each IgG fusion using purified HLZ as a standard, and probed with goat anti-human IgG-HRP. For IgG ELISA, plates were coated with serial dilutions of extracts or human IgG standard and probed with goat anti-human IgG-HRP. For gel quantification, ImageJ software was used to compare the IgG fusion band intensity visualized on stain-free polyacrylamide gels using purified 6D8 antibody as standard. Columns represent means ± standard error from three independently infiltrated leaf samples **(B)**. Clarified leaf extracts were separated by reducing SDS-PAGE and a representative gel image is shown. The general band position corresponding to each respective heavy chain/ZE3 fusion is indicated "ZH/HZ." The small shift in size in HLZe (~67 kDa of the reduced heavy chain fusion before glycosylation) and HLZd (~65 kDa) or HLZ (~64.5 kDa) is due to epitope tag truncation. ZH and ZHx have a predicted size of ~64.5 kDa. The "<" indicates ZE3-Fc (~40 kDa) and Fc (~29 kDa) fragments. The large subunit of Rubisco is abbreviated "RbcL".
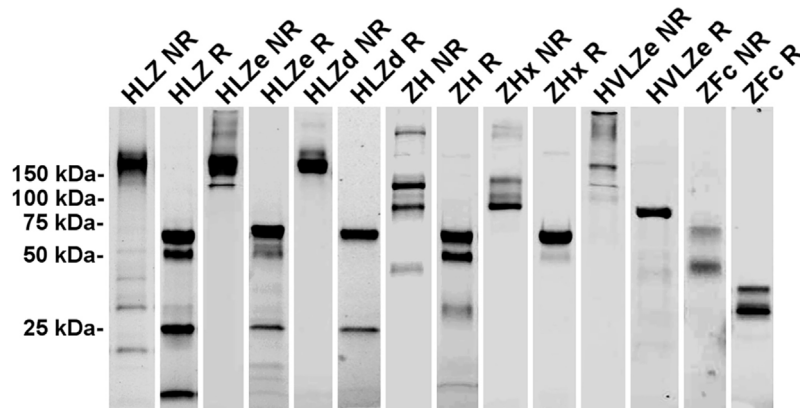
FIGURE 3 | Purification of IgG fusions. Agroinfiltrated leaf material between 1 and 3 plants per construct was homogenized, clarified, and purified by protein G affinity chromatography. The peak elutions were pooled and separated on nonreducing (NR) and reducing (R) SDS-PAGE using stain-free polyacrylamide gels. Representative lanes for each construct are compiled from multiple gels here.

sedimentation. Consistent with the formation of large immune complexes, HLZe and HVLZe were found mostly in the bottom of the gradient while HLZ, ZH, and ZFc were found mostly at the top of the gradient (**Figures 4A, B**). A small shift in density was noted with construct HLZ (**Figure 4A**) compared to unfused HL, which may explain the increased C1q binding (**Figure 1B**). Soluble extracts of ZHx contained both low-density material as well as some very high-density material, suggesting that the combination of light chain removal and RGY mutations contributes to the formation of larger aggregates (**Figure 4B**). Extracts of HLZd showed intermediate density compared

to HLZ and HLZe (**Figure 4A**) which, when taken together with the expression data and C1q binding, are consistent with HLZd forming smaller, more soluble immune complexes compared to HLZe.

Polymeric Constructs Have Improved Stability

Producing vaccines which are stable at refrigerated temperatures, ambient temperatures, and after freeze/thawing, is a major challenge of the vaccine industry (44). First, the stability of each construct was analyzed by comparing fully formed
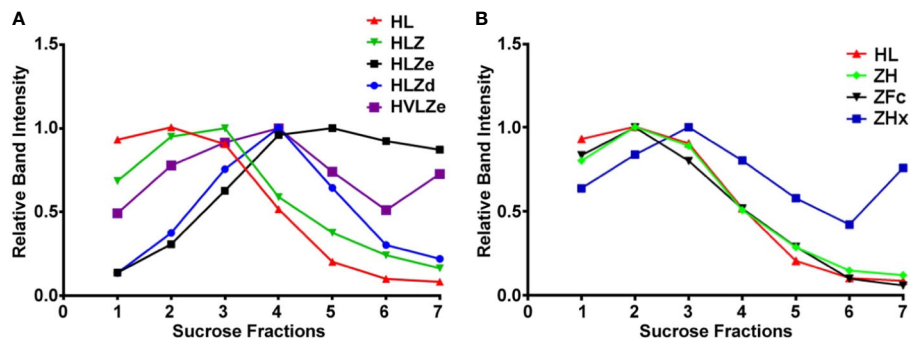
FIGURE 4 | Sucrose gradient centrifugation of IgG fusions. Purified IgG fusions were separated by sucrose gradient sedimentation using 5/10/15/20/25% discontinuous sucrose layers. Gradient fractions were analyzed by SDS-PAGE and representative results are shown; direction of sedimentation is left to right. The relative band intensity was quantified using ImageJ software and the peak band was arbitrarily assigned the value of 1. Sedimentation profiles were plotted on two separate graphs. **(A)** constructs HL, HLZ, HLZe, HLZd, and HVLZe. **(B)** constructs HL, ZH, ZFc, and ZHx. The plot for HL represents the same data for both **(A, B)**.

products and degradation products on SDS-PAGE gels after treatment with various temperature conditions. The initial level of degradation, which corresponds to any degradation that occurred during expression, purification, or the initial freeze/thaw, was substantially reduced (20–40% more fully formed product) in polymeric constructs when compared to monomeric constructs (**Figure 5A**). After five freeze-thaw cycles or two weeks at 4°C, small amounts of degradation (2–5%) were observed with all constructs (**Figure 5A**). High concentrations (>1 mg/ml) of HLZe and HVLZe precipitated after several days at 4°C (data not shown), probably due to the formation of very large insoluble complexes, thereby highlighting the undesirability of these constructs. At room temperature, most constructs had 10% and 15% degradation after two weeks (**Figure 5A**). Overall, the polymeric constructs retained the highest stability, while the monomeric constructs, and especially the Fc fusion, degraded more rapidly (**Figure 5A**).

Second, we determined whether storage resulted in an impairment of C1q binding. Most constructs retained strong C1q binding after storage; however, after room temperature storage, repeated freeze-thaw cycles, but not 4°C storage, construct HLZ unexpectedly displayed increased C1q binding (**Figure 5B**). This may be due to aggregation, degradation of the Fab regions, or loss of light chain as numerous degradation products are visible on SDS-PAGE (**Figure 3**). Conversely, construct ZFc lost C1q binding ability as it became more degraded, especially after freeze-thaw cycles, suggesting degradation of the Fc binding region (**Figure 5B**). Taken together with the expression data, constructs with intermediate levels of self-binding (e.g. HLZd and ZHx) showed the highest stability during both extraction and storage while maintaining high solubility. Of these, only construct HLZd could be produced at high levels.

IgG Fusion Enhances ZE3 Immunogenicity

IgG fusions have strong immunological properties even in the absence of adjuvant due to their improved binding of C1q and uptake *via* FcRn and Fc receptors on antigen presenting cells (11). To investigate the immunogenicity of the IgG fusions created here, BALB/c mice (n = 6) were immunized subcutaneously, without adjuvant, with two doses of each IgG fusion construct such that each

dose of ZE3 delivered was 8 μg. As a control, mice were also immunized with 8 μg His-tagged plant-expressed ZE3. As expected, all IgG fusions very strongly enhanced the production of ZE3-specific IgG, producing 20-fold to 150-fold higher total IgG titers than ZE3 alone (**Figure 6A**, p < 0.01 compared to ZE3). 5-fold to 10-fold higher mean titers were reached by the ZHx and ZFc constructs compared to the other constructs, though these differences were not statistically significant. The level of IgG2a antibodies were also measured because they have important antiviral effector functions (45) and are correlated with T-cell activation (46) and complement activity (8). All IgG fusions significantly enhanced the production of IgG2a compared to ZE3 alone (**Figure 6B**, p < 0.01 compared to ZE3). The construct HLZ, which displayed the lowest C1q binding (**Figure 1B**), had a significantly reduced production of IgG2a compared to most other fusions (**Figure 6B**, p < 0.05 compared to HLZ). Compared to total IgG, the relative ratio of IgG2a was lowest in the ZE3, HLZ, and ZFc groups (**Figure 6B**, see table). Sera from mice immunized with all IgG fusions neutralized ZIKV (**Figure 7**, p < 0.0001 compared to sera from PBS-injected mice). All IgG fusions elicited significantly higher neutralizing responses than His-tagged ZE3 (**Figure 7**, p < 0.024 compared to ZE3).
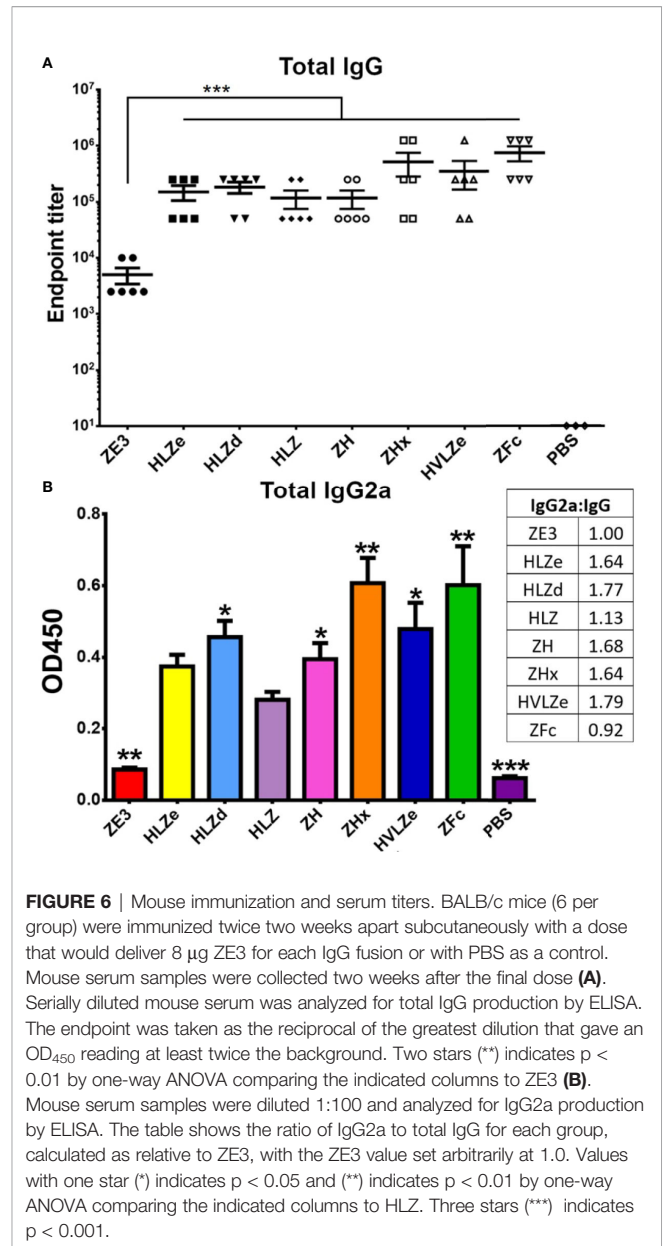
DISCUSSION

Previous work has shown that IgG fusion strategies have the potential to enhance antigen immunogenicity (18, 19, 47–49). However, the key characteristics to produce an optimal IgG fusion vaccine candidate have not been directly compared. An optimal vaccine candidate must be accessible, affordable, and stable, as well as immunogenic. Impressively, especially given the low doses and lack of adjuvant used in this study, the IgG fusions were potently immunogenic with many of the best candidates eliciting 100-fold higher antibody responses compared to antigen alone. While the highest immunological readouts were obtained by constructs ZHx and ZFc, these constructs have limited use as vaccine candidates, as ZHx suffered from low yield and aggregation, while ZFc was extraordinarily unstable prior to and during storage. These findings underscore the importance
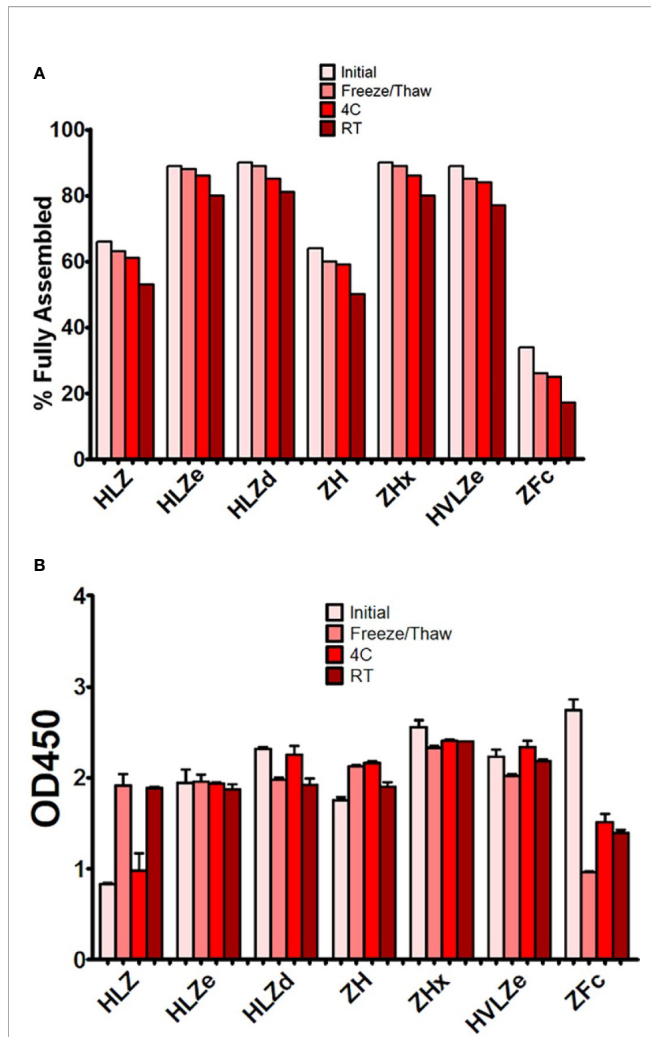
FIGURE 5 | Stability and C1q binding of purified IgG fusions. Samples of purified IgG fusions were frozen and thawed once after purification (initial), or additionally subjected to either additional five freeze/thaw cycles, incubation for 2 weeks at 4°C, or incubation for 2 weeks at 23°C **(A)**. After each treatment, samples were separated on reducing and nonreducing SDS-PAGE gels, and the relative proportion of fully assembled product was analyzed using ImageJ software. The initial measurement reflects degradation which occurred during expression or purification, whereas the other measurements reflect degradation which occurred during each respective treatment **(B)**. Samples from each treatment were analyzed by C1q binding ELISA. Columns represent the mean OD_{450} value ± standard error from three samples.

FIGURE 6 | Mouse immunization and serum titers. BALB/c mice (6 per group) were immunized twice two weeks apart subcutaneously with a dose that would deliver 8 µg ZE3 for each IgG fusion or with PBS as a control. Mouse serum samples were collected two weeks after the final dose **(A)**. Serially diluted mouse serum was analyzed for total IgG production by ELISA. The endpoint was taken as the reciprocal of the greatest dilution that gave an OD_{450} reading at least twice the background. Two stars (**) indicates $p < 0.01$ by one-way ANOVA comparing the indicated columns to ZE3 **(B)**. Mouse serum samples were diluted 1:100 and analyzed for IgG2a production by ELISA. The table shows the ratio of IgG2a to total IgG for each group, calculated as relative to ZE3, with the ZE3 value set arbitrarily at 1.0. Values with one star (*) indicates $p < 0.05$ and (**) indicates $p < 0.01$ by one-way ANOVA comparing the indicated columns to HLZ. Three stars (***) indicates $p < 0.001$.

of evaluating multiple aspects of vaccine viability. By contrast, construct HLZd had nearly double the yield of the next closest construct (**Figure 2**) while maintaining high stability (**Figure 5**), solubility (**Figure S5B**), and immunological properties (**Figures 1B**, **6**, **7**). All of the HLZd produced in this study was made in a single small *N. benthamiana* plant (data not shown), demonstrating the excellent potential of plant-based vaccine development to address vaccine affordability and accessibility. The overall properties of each construct are summarized in **Table 1**. These findings warrant further development of HLZd-like constructs as a vaccine platform which we anticipate will be

broadly applicable to the development of vaccines targeting other pathogens.

While most current antibody fusion vaccines use constructs similar to ZFc, many properties of Fc fusions, including C1q binding, vary based on the individual fusion partner and thus must be determined empirically for each fusion (41). Interestingly, some Fc fusion constructs form hexamers (50), which may explain the strong C1q binding and immunogenicity of ZFc observed here. Despite its strong immunogenicity, ZFc was remarkably unstable: ~50% of the ZE3 was proteolytically cleaved either before or during extraction (**Figures 2A, B**), even when directly extracted in SDS sample buffer or with protease inhibitors (data not shown). Further, less than 25% of full-size ZFc molecules remained intact upon repeated freeze-thaw or storage (**Figure 5A**). This degradation was associated with a loss
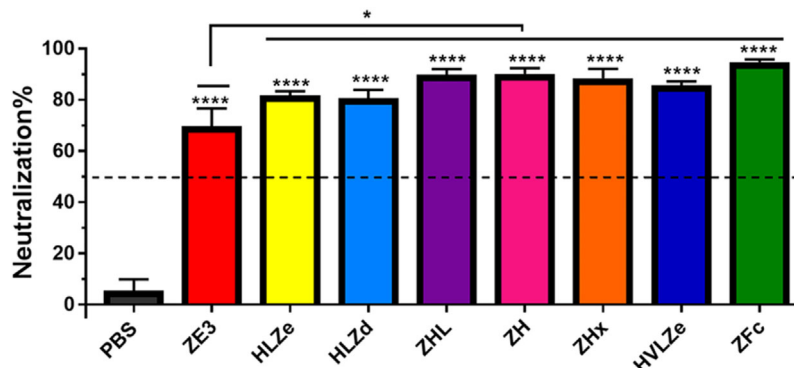
FIGURE 7 | Neutralization of ZIKV. Plaque reduction neutralization assays (PRNT) assays were performed using pooled mouse sera with dilution ratio of 1:10 to evaluate ZIKV-specific neutralizing antibodies in the sera. Data are presented as mean neutralization % and SD from three independent experiments with technical triplicates for each sample. Statistical analyses were performed using one-way ANOVA, p values from comparison between vaccine treatments and PBS were indicated with **** (<0.0001) or from comparison between vaccine treatments and His-tagged ZE3 were indicated with * (p < 0.024).

TABLE 1 | Summary of characteristics of IgG fusions.

Construct	Yield	Solubility	Sedimentation	Stability	C1q	IgG	IgG2a	Neutralization
ZE3	N.D.	N.D.	N.D.	N.D.	N.D.	+	+	++
HLZe	0.22 mg/g	Low	+++++	High	+++	+++	++	+++
HLZd	1.50 mg/g	High	+++	High	+++	+++	+++	+++
HLZ	0.17 mg/g	High	++	Medium	+	+++	++	+++
ZH	0.83 mg/g	High	+	Medium	++	+++	+++	+++
ZHx	0.21 mg/g	Low	+++*	High	+++	+++	++++	+++
VHLZe	<0.1 mg/g	Low	+++++	High	+++	+++	+++	+++
ZFc	0.57 mg/g	High	+	Low	+++	+++	++++	+++

A summary of the characteristics of each IgG fusion vaccine candidate is given. For expression, only the yield (mg/g LFW) of the fully assembled product is shown. A greater number of "+" symbols indicates either a statistically significant increase in the mean value for that property (for C1q, IgG, IgG2a, and neutralization), or a repeatedly observed difference (for sedimentation). For ZHx (*), peaks of both low- and high-velocity sedimentation were observed.

in C1q binding (**Figure 5B**), probably due to impairment of the Fc receptor binding domains. ZFc has fewer disulfide bonds than whole IgG, and in general Fc fusions often suffer from instability or undesirable aggregation (51). Further protein engineering, including optimization of linkers, may improve the stability and expression of these constructs. In contrast, IgG fusions displaying self-binding properties, such as HLZd, HLZe, and ZHx, were much more stable during extraction and storage. Consistent with their reduced binding to antibody probes during ELISA (**Figure 2A**), the intramolecular and intermolecular associations of these constructs may protect them from proteolysis or other degradative processes.

The large complex size generated by traditional RIC (i.e. HLZe) renders them poorly soluble upon extraction [**Figures 2A, S2**, (26)] with concentrations above 1 to 2 mg/ml precipitating during storage (data not shown). Therefore, we reduced the binding affinity of the RIC by mutating the 6D8 epitope tag (construct HLZd). Using this strategy of modifying the strength of self-binding, RIC can be customized to create complexes of different sizes. These findings will allow future investigation of the immunological and functional properties conferred by variably sized immune complexes. While traditional RIC require co-expression of both the heavy and light chains, this can be simplified by creating a single chain

antibody with the variable light domain fused to the variable heavy domain, as in construct HVLZe. This construct had high stability (**Figure 5**) and immunogenicity (**Figure 6**), but was poorly soluble, resulting in low recovery (**Figure 2**). By further reducing the epitope binding of HVLZe or by altering the relative positions of the light chain or antigen fusions, or by using the shorter "d" epitope tag, it is likely the solubility can be improved.

The glycosylation state of the Fc strongly controls its function and can enhance or inhibit binding to immune receptors by modulating the stability, conformation, and aggregation of the Fc (52). These alterations result in important differences in antibody effector functions, including antibody-dependent cellular cytotoxicity, antibody-dependent cell-mediated phagocytosis, complement-dependent cytotoxicity, and antibody-dependent enhancement of viral infection (53). Advances in glycoengineering have allowed targeted optimization of the Fc glycosylation state in a variety of recombinant expression systems (38, 54, 55). For example, an anti-CD20 antibody produced in glycoengineered plants lacking core xylose and fucose N-linked glycans showed improved binding to FcγRI, FcγRIIIa, and C1q (56). Similarly, anti-DENV antibodies produced in glycoengineered plants have been shown to have diminished ADE activity and, consequently, have superior efficacy and safety profiles than their mammalian cell-

produced counterparts (35). Antibody therapeutics made in glycoengineered plants have also been used to successfully treat rhesus macaques and humans with Ebola (57–60), HIV (61–63), and Chikungunya virus disease (64). In agreement with these studies, we found that C1q binding was enhanced in glycoengineered plants in a manner which acted synergystically with immune complex formation (**Figure S1**). As the entire mamallian sialylation pathway has been reconsistuted in glycoengineered plants (65), and sialylated immune complexes yield higher affinity antibodies (17), the IgG fusion vaccines used in this study may be improved by further glycan modification.

Despite its theoretically monomeric nature, construct HLZ elicited high titers and comparable neutralization to the more polymeric constructs. HLZ produced a small but repeatable improvement in C1q binding (**Figure 1B**) and a shift in small shift in density (**Figure 4A**, compare HL and HLZ) which may suggest some low-level aggregation due to the ZE3 fusion. Nonetheless, the expression of HLZ was generally low, suggesting C-terminal ZE3 fusion may interfere with proper folding or otherwise cause instability (**Figure 2A**). Many degradation products are visible by SDS-PAGE following purification (**Figure 3**) and, interestingly, the C1q binding of HLZ continued to increase upon further degradation by incubation for 2 weeks at RT or repeated freeze-thaw cycles (**Figure 5B**). These data suggest that the degradation products may be more highly immunogenic than the original construct, as light chain or Fab removal strongly improves C1q binding (**Figure S2**). This finding may have also contributed to the relatively high immunogenicity produced by HLZ (**Figure 6A**). However, despite similar total IgG titers and ZIKV neutralization, the relative IgG2a ratio was significantly reduced for HLZ, ZE3, and ZFc when compared to the more polymeric constructs (**Figure 6B**). Since IgG2a antibodies are a general indicator of a Th1 response (46) and complement activation is involved in T-cell immunity (8), these constructs may have reduced T-cell activation compared to more polymeric constructs. This is important because T-cell activation and complement activation are vital components to generate long-term B-cell immunity (8, 66). *In vitro* neutralization (**Figure 7**) does not account for antibody subclass effector functions (e.g. IgG2a) or cellular immunity, thus further investigations are warranted.

Another point to consider is that, at least for certain antibody/antigen combinations, antigen binding induces conformational changes in IgG, resulting in improved hexamer formation and subsequently improved C1q binding (40). Mixing 6D8 with an antigen containing the 6D8 epitope produced only a small increase in C1q binding (**Figure S2**). However, antigen fusion to the 6D8 N-terminus had a more pronounced effect on C1q binding (**Figure 1**), perhaps by strongly inducing conformational changes similar to antigen binding which allow hexamer formation (39). In general, we have found that antigen fusion to the 6D8 N-terminus greatly enhances C1q binding for a variety of large and small antigens (data not shown). Furthermore, removal of the 6D8 light chain (construct ZH) also substantially enhanced C1q binding (**Figure 1**). These findings agree with the hypothesis that the Fab portions of the antibody plays a regulatory role in C1q binding. Additionally, removal of the light chain may also impact glycosylation and thus C1q binding (67).

In summary, we have developed a cheap, fast, and efficient plant expression system to produce and purify high levels of IgG fusion vaccine candidates. Plant recombinant expression systems are particularly well suited to make IgG fusion vaccines, such as the ones described in this study, since they have inherent safety, high scalability, and low production costs when compared to mammalian cell systems (68–71). These benefits can be of special value for vaccine production in developing countries (72). By directly comparing many different IgG fusion strategies, we have identified a self-assembling immune complex construct HLZd that is highly expressing, stable, soluble, and immunogenic. These studies warrant future research in animal models, and we anticipate our findings will be broadly applicable to other vaccine antigens or antibody-based therapeutics.

DATA AVAILABILITY STATEMENT

The raw data supporting the conclusions of this article will be made available by the authors, without undue reservation.

ETHICS STATEMENT

The animal study was reviewed and approved by Institutional Animal Care and Use Committee at Arizona State University.

AUTHOR CONTRIBUTIONS

AD and HM designed experiments and analyzed data. AD, HM, and MP constructed vectors. AD performed C1q binding, solubility, sucrose gradient, and expression experiments. AD, JH, and MP performed purification experiments. AD and JH performed stability experiments. JK performed mouse immunization and bleeds. AD and MP performed antibody titer experiments. HS performed ZIKV neutralization experiments. MP performed FcγRIII binding experiments. AD wrote the manuscript. AD, HM, and QC critically revised the MS. All authors contributed to the article and approved the submitted version.

FUNDING

SUPPLEMENTARY MATERIAL

The Supplementary Material for this article can be found online at: https://www.frontiersin.org/articles/10.3389/fimmu.2020.576012/full#supplementary-material

REFERENCES

1. Reed SG, Orr MT, Fox CB. Key roles of adjuvants in modern vaccines. *Nat Med* (2013) 19:1597–608. doi: 10.1038/nm.3409

2. Carter PJ. Introduction to current and future protein therapeutics: A protein engineering perspective. *Exp Cell Res* (2011) 317:1261–9. doi: 10.1016/j.yexcr.2011.02.013

3. Roopenian DC, Akilesh S. FcRn: the neonatal Fc receptor comes of age. *Nat Rev Immunol* (2007) 7:715–25. doi: 10.1038/nri2155

4. Qiao SW, Kobayashi K, Johansen FE, Sollid LM, Andersen JT, Milford E, et al. Dependence of antibody-mediated presentation of antigen on FcRn. *Proc Natl Acad Sci U.S.A.* (2008) 105:9337–42. doi: 10.1073/pnas.0801717105

5. Baker K, Qiao SW, Kuo TT, Aveson VG, Platzer B, Andersen JT, et al. Neonatal Fc receptor for IgG (FcRn) regulates cross-presentation of IgG immune complexes by CD8-CD11b+ dendritic cells. *Proc Natl Acad Sci U.S.A.* (2011) 108:9927–32. doi: 10.1073/pnas.1019037108

6. Fletcher EAK, van Maren W, Cordfunke R, Dinkelaar J, Codee JDC, van der Marel G, et al. Formation of Immune Complexes with a Tetanus-Derived B Cell Epitope Boosts Human T Cell Responses to Covalently Linked Peptides in an Ex Vivo Blood Loop System. *J Immunol* (2018) 201:87–97. doi: 10.4049/jimmunol.1700911

7. McCloskey ML, Curotto De Lafaille MA, Carroll MC, Erlebacher A. Acquisition and presentation of follicular dendritic cell-bound antigen by lymph node-resident dendritic cells. *J Exp Med* (2011) 208:135–48. doi: 10.1084/jem.20100354

8. West EE, Kolev M, Kemper C. Complement and the Regulation of T Cell Responses. *Annu Rev Immunol* (2018) 36:309–38. doi: 10.1146/annurev-immunol-042617-053245

9. Bournazos S, Ravetch JV. Fcγ Receptor Function and the Design of Vaccination Strategies. *Immunity* (2017) 47:224–33. doi: 10.1016/j.immuni.2017.07.009

10. Vidarsson G, Dekkers G, Rispens T. IgG subclasses and allotypes: From structure to effector functions. *Front Immunol* (2014) 5:520. doi: 10.3389/fimmu.2014.00520

11. Czajkowsky DM, Hu J, Shao Z, Pleass RJ. Fc-fusion proteins: New developments and future perspectives. *EMBO Mol Med* (2012) 4:1015–28. doi: 10.1002/emmm.201201379

12. Ho NI, Camps MGM, de Haas EFE, Trouw LA, Verbeek JS, Ossendorp F. C1q-Dependent Dendritic Cell Cross-Presentation of In Vivo-Formed Antigen-Antibody Complexes. *J Immunol* (2017) 198:4235–43. doi: 10.4049/jimmunol.1602169

13. Getahun A, Heyman B. How antibodies act as natural adjuvants. *Immunol Lett* (2006) 104:38–45. doi: 10.1016/j.imlet.2005.11.005

14. van Montfoort N, Mangsbo SM, Camps MGM, van Maren WWC, Verhaart IEC, Waisman A, et al. Circulating specific antibodies enhance systemic cross-priming by delivery of complexed antigen to dendritic cells in vivo. *Eur J Immunol* (2012) 42:598–606. doi: 10.1002/eji.201141613

15. Tsouchnikas G, Zlatkovic J, Jarmer J, Strauß V, Vratskikh O, Kundi M, et al. Immunization with Immune Complexes Modulates the Fine Specificity of Antibody Responses to a Flavivirus Antigen. *J Virol* (2015) 89:7970–8. doi: 10.1128/JVI.00938-15

16. Hioe CE, Kumar R, Upadhyay C, Jan M, Fox A, Itri V, et al. Modulation of Antibody Responses to the V1V2 and V3 Regions of HIV-1 Envelope by Immune Complex Vaccines. *Front Immunol* (2018) 9:2441:2441. doi: 10.3389/fimmu.2018.02441

17. Maamary J, Wang TT, Tan GS, Palese P, Ravetch JV. Increasing the breadth and potency of response to the seasonal influenza virus vaccine by immune complex immunization. *Proc Natl Acad Sci U S A* (2017) 114:10172–7. doi: 10.1073/pnas.1707950114

18. Webster GR, van Dolleweerd C, Guerra T, Stelter S, Hofmann S, Kim MY, et al. A polymeric immunoglobulin—antigen fusion protein strategy for enhancing vaccine immunogenicity. *Plant Biotechnol J* (2018) 16:1983–96. doi: 10.1111/pbi.12932

19. Kim MY, Copland A, Nayak K, Chandele A, Ahmed MS, Zhang Q, et al. Plant-expressed Fc-fusion protein tetravalent dengue vaccine with inherent adjuvant properties. *Plant Biotechnol J* (2018) 16:1283–94. doi: 10.1111/pbi.12869

20. Mason HS. Recombinant immune complexes as versatile and potent vaccines. *Hum Vaccin Immunother* (2016) 12:988–9. doi: 10.1080/21645515.2015.1116655

21. Chargelegue D, Drake PMW, Obregon P, Prada A, Fairweather N, Ma JKC. Highly immunogenic and protective recombinant vaccine candidate expressed in transgenic plants. *Infect Immun* (2005) 73:5915–22. doi: 10.1128/IAI.73.9.5915-5922.2005

22. Phoolcharoen W, Bhoo SH, Lai H, Ma J, Arntzen CJ, Chen Q, et al. Expression of an immunogenic Ebola immune complex in Nicotiana benthamiana. *Plant Biotechnol J* (2011) 9:807–16. doi: 10.1111/j.1467-7652.2011.00593.x

23. Phoolcharoen W, Dye JM, Kilbourne J, Piensook K, Pratt WD, Arntzen CJ, et al. A nonreplicating subunit vaccine protects mice against lethal Ebola virus challenge. *Proc Natl Acad Sci U.S.A.* (2011) 108:20695–700. doi: 10.1073/pnas.1117715108

24. Pepponi I, Diogo GR, Stylianou E, van Dolleweerd CJ, Drake PMW, Paul MJ, et al. Plant-derived recombinant immune complexes as self-adjuvanting TB immunogens for mucosal boosting of BCG. *Plant Biotechnol J* (2014) 12:840–50. doi: 10.1111/pbi.12185

25. Kim M-Y, Reljic R, Kilbourne J, Ceballos-Olvera I, Yang M-S, Reyes-del Valle J, et al. Novel vaccination approach for dengue infection based on recombinant immune complex universal platform. *Vaccine* (2015) 33:1830–8. doi: 10.1016/j.vaccine.2015.02.036

26. Diamos AG, Larios D, Brown L, Kilbourne J, Kim HS, Saxena D, et al. Vaccine synergy with virus-like particle and immune complex platforms for delivery of human papillomavirus L2 antigen. *Vaccine* (2019) 37:137–44. doi: 10.1016/j.vaccine.2018.11.021

27. Diamos AG, Pardhe MD, Sun H, Hunter JGL, Mor T, Meador L, et al. Codelivery of improved immune complex and virus-like particle vaccines containing Zika virus envelope domain III synergistically enhances immunogenicity. *Vaccine* (2020) 38:3455–63. doi: 10.1016/j.vaccine.2020.02.089

28. Shukla R, Shanmugam RK, Ramasamy V, Arora U, Batra G, Acklin JA, et al. Zika virus envelope nanoparticle antibodies protect mice without risk of disease enhancement. *EBioMedicine* (2020) 54:102738. doi: 10.1016/j.ebiom.2020.102738

29. Stettler K, Beltramello M, Espinosa DA, Graham V, Cassotta A, Bianchi S, et al. Specificity, cross-reactivity, and function of antibodies elicited by Zika virus infection. *Sci (80)* (2016) 353:823–6. doi: 10.1126/science.aaf8505

30. Yang M, Dent M, Lai H, Sun H, Chen Q. Immunization of Zika virus envelope protein domain III induces specific and neutralizing immune responses against Zika virus. *Vaccine* (2017) 35:4287–94. doi: 10.1016/j.vaccine.2017.04.052

31. Diamos AG, Hunter JGL, Pardhe MD, Rosenthal SH, Sun H, Foster BC, et al. High Level Production of Monoclonal Antibodies Using an Optimized Plant Expression System. *Front Bioeng Biotechnol* (2020) 7:472:472. doi: 10.3389/fbioe.2019.00472

32. Huang Z, Mason HS. Conformational analysis of hepatitis B surface antigen fusions in an Agrobacterium-mediated transient expression system. *Plant Biotechnol J* (2004) 2:241–9. doi: 10.1111/j.1467-7652.2004.00068.x

33. Castilho A, Steinkellner H. Glyco-engineering in plants to produce human-like N-glycan structures. *Biotechnol J* (2012) 7:1088–98. doi: 10.1002/biot.201200032

34. Santi L, Batchelor L, Huang Z, Hjelm B, Kilbourne J, Arntzen CJ, et al. An efficient plant viral expression system generating orally immunogenic Norwalk virus-like particles. *Vaccine* (2008) 26:1846–54. doi: 10.1016/j.vaccine.2008.01.053

35. Dent M, Hurtado J, Paul AM, Sun H, Lai H, Yang M, et al. Plant-produced anti-dengue virus monoclonal antibodies exhibit reduced antibody-dependent enhancement of infection activity. *J Gen Virol* (2016) 97:3280–90. doi: 10.1099/jgv.0.000635

36. Croix DA, Ahearn JM, Rosengard AM, Han S, Kelsoe G, Ma M, et al. Antibody response to a T-dependent antigen requires B cell expression of complement receptors. *J Exp Med* (1996) 183:1857–64. doi: 10.1084/jem.183.4.1857

37. Phan TG, Grigorova I, Okada T, Cyster JG. Subcapsular encounter and complement-dependent transport of immune complexes by lymph node B cells. *Nat Immunol* (2007) 8:992–1000. doi: 10.1038/ni1494

38. Kallolimath S, Steinkellner H. Glycosylation of plant produced human antibodies. *Hum Antibodies* (2015) 23:45–8. doi: 10.3233/HAB-150283

39. Diebolder CA, Beurskens FJ, de Jong RN, Koning RI, Strumane K, Lindorfer MA, et al. Complement Is Activated by IgG Hexamers Assembled at the Cell Surface. *Sci (80)* (2014) 343:1260–3. doi: 10.1126/science.1248943

40. Wang G, de Jong RN, van den Bremer ETJ, Beurskens FJ, Labrijn AF, Ugurlar D, et al. Molecular Basis of Assembly and Activation of Complement Component C1 in Complex with Immunoglobulin G1 and Antigen. *Mol Cell* (2016) 63:135–45. doi: 10.1016/J.MOLCEL.2016.05.016

41. Lagassé HAD, Hengel H, Golding B, Sauna ZE. Fc-Fusion Drugs Have FcγR/C1q Binding and Signaling Properties That May Affect Their Immunogenicity. *AAPS J* (2019) 21:62. doi: 10.1208/s12248-019-0336-8

42. Wilson JA, Hevey M, Bakken R, Guest S, Bray M, Schmaljohn AL, et al. Epitopes involved in antibody-mediated protection from Ebola virus. *Sci (80)* (2000) 287:1664–6. doi: 10.1126/science.287.5458.1664

43. Thielens NM, Tedesco F, Bohlson SS, Gaboriaud C, Tenner AJ. C1q: A fresh look upon an old molecule. *Mol Immunol* (2017) 89:73–83. doi: 10.1016/j.molimm.2017.05.025

44. Kumru OS, Joshi SB, Smith DE, Middaugh CR, Prusik T, Volkin DB. Vaccine instability in the cold chain: Mechanisms, analysis and formulation strategies. *Biologicals* (2014) 42:237–59. doi: 10.1016/j.biologicals.2014.05.007

45. Lu LL, Suscovich TJ, Fortune SM, Alter G. Beyond binding: antibody effector functions in infectious diseases. *Nat Rev Immunol* (2018) 18:46–61. doi: 10.1038/nri.2017.106

46. Huber VC, McKeon RM, Brackin MN, Miller LA, Keating R, Brown SA, et al. Distinct contributions of vaccine-induced immunoglobulin G1 (IgG1) and IgG2a antibodies to protective immunity against influenza. *Clin Vaccine Immunol* (2006) 13:981–90. doi: 10.1128/CVI.00156-06

47. Loureiro S, Ren J, Phapugrangkul P, Colaco CA, Bailey CR, Shelton H, et al. Adjuvant-Free Immunization with Hemagglutinin-Fc Fusion Proteins as an Approach to Influenza Vaccines. *J Virol* (2011) 85:3010–4. doi: 10.1128/jvi.01241-10

48. Zhao B, Zhang X, Krummenacher C, Song S, Gao L, Zhang H, et al. Immunization with Fc-based recombinant Epstein-Barr virus gp350 elicits potent neutralizing humoral immune response in a BALB/c mice model. *Front Immunol* (2018) 9:932:932. doi: 10.3389/fimmu.2018.00932

49. Konduru K, Bradfute SB, Jacques J, Manangeeswaran M, Nakamura S, Morshed S, et al. Ebola virus glycoprotein Fc fusion protein confers protection against lethal challenge in vaccinated mice. *Vaccine* (2011) 29:2968–77. doi: 10.1016/j.vaccine.2011.01.113

50. Zhang Y, Zhou Z, Zhu SL, Zu X, Wang Z, Zhang LK, et al. A novel RSV F-Fc fusion protein vaccine reduces lung injury induced by respiratory syncytial virus infection. *Antiviral Res* (2019) 165:11–22. doi: 10.1016/j.antiviral.2019.02.017

51. Zeng F, Yang C, Gao X, Li X, Zhang Z, Gong R. Comprehensive elucidation of the structural and functional roles of engineered disulfide bonds in antibody Fc fragment. *J Biol Chem* (2018) 293:19127–35. doi: 10.1074/jbc.RA118.005367

52. Mastrangeli R, Palinsky W, Bierau H. Glycoengineered antibodies: towards the next-generation of immunotherapeutics. *Glycobiology* (2019) 29:199–210. doi: 10.1093/glycob/cwy092

53. Sun H, Chen Q, Lai H. Development of antibody therapeutics against flaviviruses. *Int J Mol Sci* (2017) 19:54. doi: 10.3390/ijms19010054

54. Gupta SK, Shukla P. Glycosylation control technologies for recombinant therapeutic proteins. *Appl Microbiol Biotechnol* (2018) 102:10457–68. doi: 10.1007/s00253-018-9430-6

55. Wang Q, Chung C-Y, Chough S, Betenbaugh MJ. Antibody glycoengineering strategies in mammalian cells. *Biotechnol Bioeng* (2018) 115:1378–93. doi: 10.1002/bit.26567

56. Marusic C, Pioli C, Stelter S, Novelli F, Lonoce C, Morrocchi E, et al. Donini M. N-glycan engineering of a plant-produced anti-CD20-hIL-2 immunocytokine significantly enhances its effector functions. *Biotechnol Bioeng* (2018) 115:565–76. doi: 10.1002/bit.26503

57. Qiu X, Wong G, Audet J, Bello A, Fernando L, Alimonti JB, et al. Reversion of advanced Ebola virus disease in nonhuman primates with ZMapp. *Nature* (2014) 514:47–53. doi: 10.1038/nature13777

58. Zeitlin L, Pettitt J, Scully C, Bohorova N, Kim D, Pauly M, et al. Enhanced potency of a fucose-free monoclonal antibody being developed as an Ebola virus immunoprotectant. *Proc Natl Acad Sci* (2011) 108:20690–4. doi: 10.1073/pnas.1108360108

59. Lyon GM, Mehta AK, Varkey JB, Brantly K, Plyler L, McElroy AK, et al. Clinical care of two patients with Ebola virus disease in the United States. *N Engl J Med* (2014) 371:2402–9. doi: 10.1056/NEJMoa1409838

60. Olinger GG, Pettitt J, Kim D, Working C, Bohorov O, Bratcher B, et al. Delayed treatment of Ebola virus infection with plant-derived monoclonal antibodies provides protection in rhesus macaques. *Proc Natl Acad Sci U.S.A.* (2012) 109:18030–5. doi: 10.1073/pnas.1213709109

61. Forthal DN, Gach JS, Landucci G, Jez J, Strasser R, Kunert R, et al. Fc-Glycosylation Influences Fcγ Receptor Binding and Cell-Mediated Anti-HIV Activity of Monoclonal Antibody 2G12. *J Immunol* (2010) 185:6876–82. doi: 10.4049/jimmunol.1002600

62. Ma JKC, Drossard J, Lewis D, Altmann F, Boyle J, Christou P, et al. Regulatory approval and a first-in-human phase I clinical trial of a monoclonal antibody produced in transgenic tobacco plants. *Plant Biotechnol J* (2015) 13:1106–20. doi: 10.1111/pbi.12416

63. Stelter S, Paul MJ, Teh AYH, Grandits M, Altmann F, Vanier J, et al. Engineering the interactions between a plant-produced HIV antibody and human Fc receptors. *Plant Biotechnol J* (2020) 18:402–14. doi: 10.1111/pbi.13207

64. Hurtado J, Acharya D, Lai H, Sun H, Kallolimath S, Steinkellner H, et al. In vitro and in vivo efficacy of anti-chikungunya virus monoclonal antibodies produced in wild-type and glycoengineered Nicotiana benthamiana plants. *Plant Biotechnol J* (2020) 18:266–73. doi: 10.1111/pbi.13194

65. Castilho A, Neumann L, Daskalova S, Mason HS, Steinkellner H, Altmann F, et al. Engineering of sialylated mucin-type O-glycosylation in plants. *J Biol Chem* (2012) 287:36518–26. doi: 10.1074/jbc.M112.402685

66. Akkaya M, Kwak K, Pierce SK. B cell memory: building two walls of protection against pathogens. *Nat Rev Immunol* (2020) 20:229–38. doi: 10.1038/s41577-019-0244-2

67. He J, Lai H, Engle M, Gorlatov S, Gruber C, Steinkellner H, et al. Generation and Analysis of Novel Plant-Derived Antibody-Based Therapeutic Molecules against West Nile Virus. *PloS One* (2014) 9:e93541. doi: 10.1371/journal.pone.0093541

68. Alam A, Jiang L, Kittleson GA, Steadman KD, Nandi S, Fuqua JL, et al. Technoeconomic Modeling of Plant-Based Griffithsin Manufacturing. *Front Bioeng Biotechnol* (2018) 6:102:102. doi: 10.3389/fbioe.2018.00102

69. Buyel JF. Plant molecular farming – Integration and exploitation of side streams to achieve sustainable biomanufacturing. *Front Plant Sci* (2019) 9:1893. doi: 10.3389/fpls.2018.01893

70. Gleba YY, Tusé D, Giritch A. Plant viral vectors for delivery by Agrobacterium. *Curr Top Microbiol Immunol* (2014) 375:155–92. doi: 10.1007/82_2013_352

71. Chen Q, Davis KR. The potential of plants as a system for the development and production of human biologics. *F1000Research* (2016) 5:912. doi: 10.12688/f1000research.8010.1

72. Ma JKC, Christou P, Chikwamba R, Haydon H, Paul M, Ferrer MP, et al. Realising the value of plant molecular pharming to benefit the poor in developing countries and emerging economies. *Plant Biotechnol J* (2013) 11:1029–33. doi: 10.1111/pbi.12127